Martini *et al. BMC Methods* (2026) 3:21
https://doi.org/10.1186/s44330-026-00074-7

BMC Methods

PROTOCOL Open Access

Real-time monitoring of protein self-assembly by dynamic light scattering

Maria Alessandra Martini[1], Astrid Winterhalter[1], Annika J. Weber[1], Jennifer Kühne[1], Julian S. Hertel[1], Kersten S. Rabe[1] and Christof M. Niemeyer[1*]

Abstract

Background Dynamic light scattering (DLS) is a widely accessible technique for determining particle size distributions in solution. Although most commonly used to characterize samples at equilibrium, DLS can also provide insight into dynamic processes. Here, we present a protocol that employs DLS for real-time monitoring of protein self-assembly, enabling quantitative characterization of assembly kinetics. We have applied this approach to enzyme-based nanogels and hydrogels for biocatalytic applications, and it can be readily extended to other self-assembling biomolecular systems.

Methods The protocol comprises four main components: (1) preparation and quality control of individual proteins; (2) initiation of the self-assembly reaction coupled with continuous DLS measurements; (3) time-resolved control measurements of the individual proteins; and (4) evaluation and analysis of the resulting data to extract growth profiles and assess assembly dynamics. All measurements and metadata are organized in a FAIR-compliant research data management workflow, enabling transparent analysis and long-term reuse of time-resolved DLS datasets.

Results The protocol provides time-resolved hydrodynamic diameters with a temporal resolution on the order of minutes. It requires only small sample volumes and a standard benchtop DLS instrument. From sample preparation to data visualization and deposition, the complete workflow can be completed within approximately 8 h.

Conclusions This protocol enables robust, real-time monitoring of protein self-assembly and provides quantitative insights into the kinetics and performance of self-assembling systems. The integration of FAIR research data management facilitates reproducibility and comparative analysis across proteins, variants, and experimental conditions.

Keywords Dynamic light scattering, Protein self-assembly, Enzyme hydrogels, Real-time monitoring, Hydrodynamic diameter, Self-assembling biomaterials, Biocatalysis, FAIR data management

*Correspondence:
Christof M. Niemeyer
niemeyer@kit.edu
[1]Institute for Biological Interfaces 1 (IBG-1), Karlsruhe Institute of Technology (KIT), Hermann-von-Helmholtz-Platz 1, D-76344 Eggenstein-Leopoldshafen, Germany

Background

Self-assembled protein-based materials have emerged as a versatile class of biomaterials with broad applications in biosensing, biomedicine, food technology, and industrial catalysis [1, 2]. Their intrinsic biocompatibility and structural tunability make them valuable building blocks for functional materials. A central challenge across these applications lies in engineering assemblies with defined structure, stability, and functionality.

In industrial biocatalysis, protein assemblies are of particular interest due to their potential to support sustainable and efficient chemical production [3–6]. Flow biocatalytic processes increasingly rely on gentle yet stable enzyme immobilization strategies [7–10]. Inspired by natural enzyme organization, protein fusions and synthetic scaffolds have been developed to improve multi-enzyme catalysis, although issues such as uncontrolled aggregation continue to highlight the need for more robust, self-assembling systems [11, 12].

To address these challenges, we have developed all-enzyme hydrogels (AEHs) [13] based on covalent SpyCatcher/SpyTag (SC/ST) conjugation [14]. These materials form dense yet hydrated three-dimensional networks through spontaneous isopeptide bond formation, enabling highly robust assemblies with controlled stoichiometry and mechanical stability. As illustrated in Fig. 1a, complementary SC/ST-equipped enzymes crosslink into a continuous protein network that remains

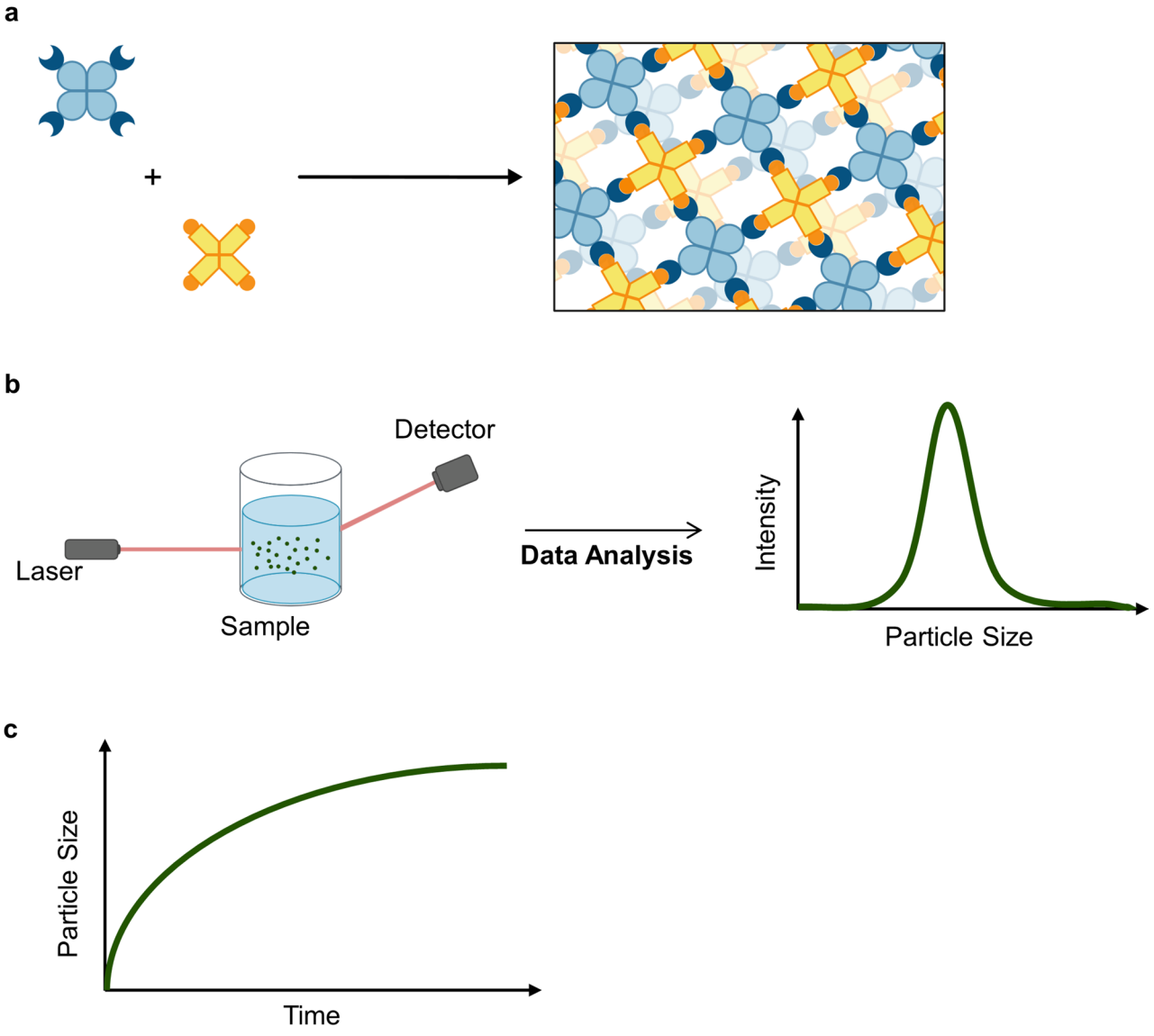

Fig. 1 (**a**) Schematic representation of the formation of an all-protein hydrogel from the assembly of two tetrameric proteins genetically engineered to harbor complementary self-assembling motifs (shown in dark blue and orange). (**b**) Simplified representation of a typical DLS setup yielding intensity size distribution. (**c**) Schematic representation of the time-dependent growth of enzyme hydrogel particles (nanogels) during self-assembly.

permeable for substrates and products. In solution, the initial crosslinking of the complementary building blocks leads to the formation of nanoscale hydrogel particles ("nanogels"), which, upon concentration or drying, coalesce into continuous macroscopic hydrogels. Throughout this manuscript, the term "nanogel" is used to refer to these nanoscale assemblies detected in solution by DLS, whereas "hydrogel" denotes the corresponding macroscopic materials formed upon further concentration or processing.

The balance of structural integrity and mass transport has enabled AEHs to be implemented in durable microfluidic reactors [15–19], produced intracellularly [20], and advanced through covalent and non-covalent assembly strategies into monodisperse foam materials with excellent stability and flow performance [21, 22].

While endpoint characterization methods for protein assemblies are well established, there is a lack of straightforward techniques to monitor protein self-assembly as it occurs. This methodological gap limits mechanistic understanding, hinders optimization of assembly conditions, and complicates quality control, particularly for systems that depend on precise stoichiometry or engineered interaction modules.

Dynamic light scattering (DLS), also known as photon correlation spectroscopy or quasi-elastic light scattering, is a widely used, non-invasive technique for determining hydrodynamic particle sizes in solution. It detects time-dependent fluctuations in scattered laser light arising from the Brownian motion of particles and converts the temporal autocorrelation function into size information via established analytical models (Fig. 1b-c) [23, 24]. DLS covers a broad size range (1 nm to 10 µm) and has been applied to proteins, polymers, micelles, nanoparticles, and colloids.

Although DLS is most commonly used to assess equilibrium samples, it can also be applied to dynamic or evolving systems. DLS has also been widely used to monitor protein aggregation as a non-equilibrium process, including applications in food protein systems, studies of protein crystallizability, and the characterization of therapeutic protein formulations [25]. Previous studies have used DLS to follow DNA origami assembly [26], crystal growth [27], or fast kinetic processes using advanced modalities [28] and stopped-flow coupling [29]. The time-dependent evolution of particle size during self-assembly, conceptually shown in Fig. 1c, illustrates that DLS has inherent potential for capturing assembly kinetics. However, a standardized and broadly accessible protocol for real-time monitoring of engineered protein self-assembly under controlled conditions has been lacking.

To fill this gap, we developed a continuous DLS-based workflow that records particle growth immediately after mixing of the complementary self-assembling proteins and quantifies the evolution of the hydrodynamic diameter over time. This protocol provides mechanistic insight into protein assembly, serves as a rapid quality control tool for engineered variants, and integrates FAIR (Findable, Accessible, Interoperable, Reusable) data management to ensure transparent and reusable handling of time-resolved datasets. Together, this approach establishes an accessible and reproducible method for studying protein self-assembly kinetics and optimizing biomolecular material systems.

Applications

We applied this protocol to investigate the self-assembly of all-enzyme hydrogels (AEHs) designed for biocatalytic applications. In an initial study, DLS was used to quantify how protein concentration influences the dynamics of nanogel formation and how altering the stoichiometry of two SC/ST-interacting enzymes affects the final particle size. These effects are shown in Fig. 2a and b [13]. The resulting data enabled optimization of AEH synthesis conditions, which were subsequently implemented in continuous-flow biocatalytic reactors. In a follow-up study, the protocol was used to compare engineered protein variants carrying different numbers of self-assembling motifs and to determine the optimal molar ratios required for efficient network formation [15].

More recently, we applied DLS to analyze the assembly kinetics of proteins harboring non-covalent interaction modules, specifically PDZ, SH3, and GBD domains. The corresponding time-resolved particle growth profiles are shown in Fig. 2c-e [22]. Qualitatively consistent with their reported binding affinities (K_d approximately 8.0 µM for PDZ and approximately 0.1 µM for SH3) [30], the SH3-based system assembled more rapidly and reached a larger hydrodynamic diameter than the PDZ-based system, while both remained below the final sizes observed for the covalent SC/ST interaction shown in Fig. 2a. In contrast, the GBD system, which has an intermediate affinity (K_d approximately 1 µM), displayed a much slower increase in hydrodynamic diameter, as shown in Fig. 2e. The unexpected increase observed for one of the individual components, GDH-GBDL (turquoise curve in Fig. 2e), suggests that this protein may undergo unspecific aggregation under the assay conditions. Although the underlying cause remains unclear, this example illustrates how irregular behavior of individual assembly components, for example due to insufficient stability of the tertiary structure during prolonged incubation, can be readily detected using this protocol.

Although our applications have focused on enzyme-based systems, the procedure is readily adaptable to other self-assembling biomolecules. In our case, the analyzed

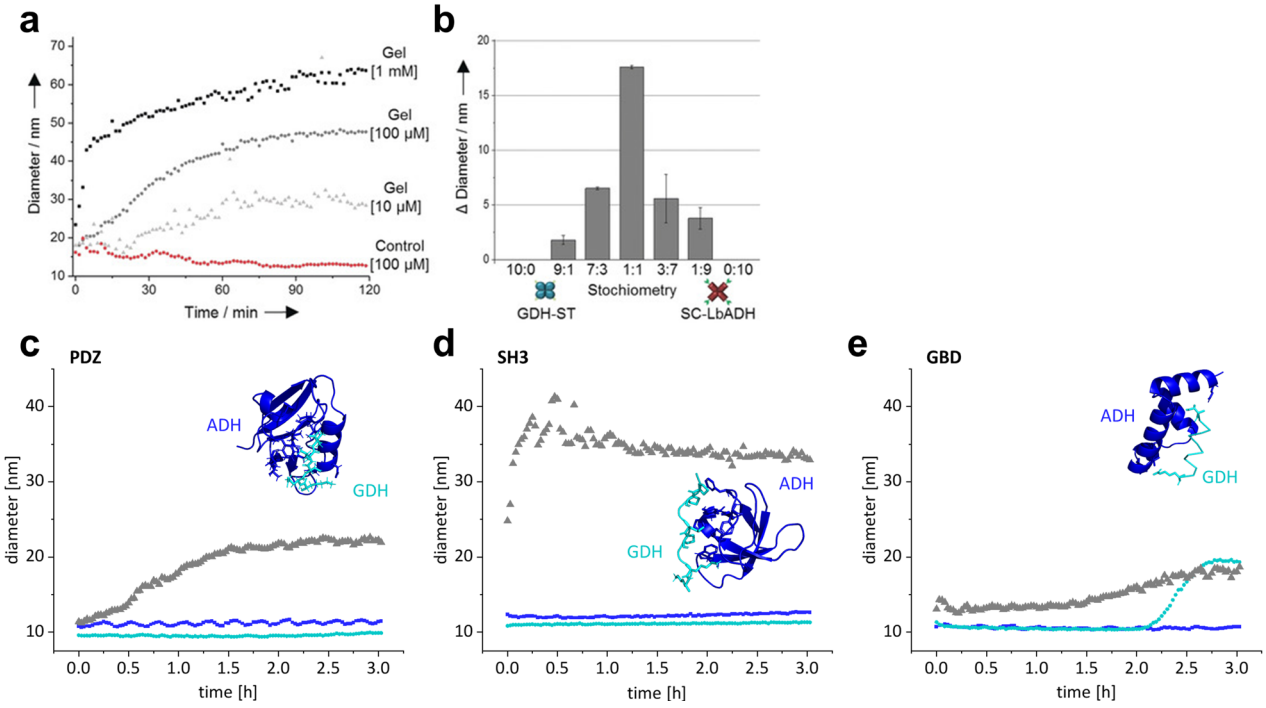

Fig. 2 Examples of the application of the DLS methodology to study self-assembling enzymes. Unless stated otherwise, particle sizes shown in this figure correspond to Z-average values obtained from monomodal (cumulant) analysis. (**a**) Time- and concentration-dependent increase in hydrodynamic diameter determined at 25 °C for the enzymes SC-LbADH and GDH-ST; the control contained equimolar amounts of GDH-ST and LbADH lacking the SC domain. (**b**) Stoichiometry-dependent increase in particle diameter observed in the first 30 min after mixing SC-LbADH and GDH-ST (100 µM total subunit concentration, 25 °C). **c**–**e**) Time-dependent nanogel formation in solution for LbADH-XB and BsGDH-XL (X = PDZ in c, X = SH3 in d, and X = GBD in e; B and L denote the binding and ligand domains of each interaction module, represented in the cartoons as dark and light blue structures, respectively) using the standardized protocol established in this work. For each sample, a total protein concentration of 0.5 mM was used, with hydrodynamic diameter (Z-average) measured every 100 s over a period of 3 h at 25 °C. The equimolar mixture of binding partners is shown in gray, and the corresponding individual proteins are shown in dark blue (binding domains) and turquoise (ligands). Initial particle growth rates calculated by linear regression of the early time points were 0.12 nm per minute in **c**), 1.97 nm per minute in **d**), and 0.06 nm per minute in **e**). Panels (**a**) and (**b**) are adapted with permission from [13], and panels **c**), **d**), and **e**) from [22].

proteins were engineered with sufficient valency to form extended three-dimensional networks that yield macroscopic hydrogels upon drying. In principle, the same workflow can also be used to study proteins that assemble into defined multimeric complexes rather than networks. Depending on the system, however, the resolution of standard benchtop DLS instruments may not always be sufficient to clearly distinguish between individual proteins and their assembled species. Given the increasing interest in recombinant biomimetic protein materials for biotechnology and biomedicine, we expect this protocol to be broadly useful for characterizing a wide variety of self-assembling systems.

Comparison to other methods

Several established techniques, such as atomic force microscopy (AFM) and transmission electron microscopy (TEM), can be used to determine particle size. However, both require extensive sample preparation, including immobilization on solid supports, and therefore provide only endpoint measurements. Other approaches for monitoring kinetics in real time, such as surface plasmon resonance (SPR) or quartz crystal microbalance with dissipation monitoring (QCM-D), are likewise surface-dependent and do not provide particle size information in solution. In contrast, our protocol relies on dynamic light scattering (DLS), which is broadly accessible, requires only a standard benchtop instrument, and enables measurements directly in solution under conditions that closely resemble both physiological environments and the synthesis of all-enzyme hydrogels. The short measurement time of DLS provides temporal resolution on the order of minutes and makes the method amenable to automation and high-throughput screening, allowing systematic evaluation of parameters such as protein concentration or buffer composition.

To benchmark our protocol against established techniques, we compared endpoint Z-average values for nanogel particles (approximately 110 nm) obtained from cell lysates by DLS with size estimates determined by AFM (distribution centered around approximately 50 nm) [20]. The values are in reasonable agreement, given

that DLS reports the hydrodynamic diameter of particles in solution, whereas AFM and TEM measure dried and immobilized samples, which typically appear smaller. It should be noted that DLS-derived Z-average values are intensity-weighted estimates and are therefore best suited for comparing relative growth trends rather than determining precise absolute particle sizes, particularly in polydisperse systems.

Despite these advantages, the protocol has limitations. DLS performs best with monodisperse samples, and scattering intensity scales with the sixth power of particle diameter, making the method extremely sensitive to aggregates or larger contaminants. In the context of nanogel formation, polydispersity is inherently introduced by conjugates of varying sizes and stoichiometries. As a consequence, datasets often yield high polydispersity indices (PDI) and may not be suitable for standard cumulant analysis (see Data Analysis and Troubleshooting). Under these conditions, DLS is most useful for following growth trends and comparing self-assembly dynamics across systems or experimental conditions. The reported sizes should therefore be interpreted as estimates rather than precise hydrodynamic radii.

In addition, the applicability of the protocol depends on both the scattering properties and the dynamic behavior of the system under investigation. Very small oligomeric assemblies or weakly scattering systems may fall below the sensitivity range of standard benchtop DLS instruments, limiting reliable size determination. Experimental conditions approaching macroscopic gelation can impair data analysis due to increased viscosity and strongly reduced diffusion, which may compromise correlation functions and fitting procedures. Conversely, very fast assembly processes may exceed the effective temporal resolution of the protocol, as manual mixing and initiation of measurements impose a lower bound on the earliest accessible time points. Under such conditions, careful optimization of protein concentration, measurement duration, and temperature is required, and complementary or faster-mixing approaches may be necessary to fully characterize the assembly process.

A further critical consideration concerns the interpretation of diffusion-based size parameters under conditions where intermolecular interactions become significant. In dilute solutions, the relationship between diffusion coefficient and hydrodynamic size is governed by the viscosity of the dispersant via the Stokes–Einstein relationship, which is assumed to remain constant during time-resolved measurements. However, at the protein concentrations used here and during self-assembly, protein–protein interactions and emerging network structures can influence diffusion behavior beyond simple solvent viscosity effects. Under such conditions, the Stokes–Einstein relationship is no longer strictly valid, and the reported size parameters do not represent true hydrodynamic radii of isolated species but rather effective, interaction-influenced diffusion properties reflecting collective behavior. Indicators of such interaction- or viscosity-related artifacts include a simultaneous increase in apparent particle size across all samples, deterioration of fit quality, or abrupt changes in correlation functions at later time points. At protein concentrations typically used here (0.5–1 mM), macroscopic gelation is not observed and such effects are generally minimal; however, at higher concentrations or advanced stages of assembly they cannot be fully excluded. In these cases, reducing protein concentration, shortening the measurement duration, or restricting data analysis to earlier time points can help mitigate such artifacts. Comparable considerations are well established in the context of diffusion interaction parameter (kD) measurements, which explicitly account for deviations from ideal dilute-solution behavior [31].

Overview of the procedure

Our protocol is organized into four main parts: (1) preparation and quality control of the individual proteins (steps 1–10); (2) continuous monitoring of the self-assembly reaction using DLS (steps 11–13); (3) time-resolved control measurements of the individual proteins (steps 14–21); and (4) evaluation and analysis of the resulting data. Together, these steps establish a reproducible workflow that enables real-time monitoring of protein self-assembly and provides an integrated quality control pipeline to assess the suitability of protein variants for hydrogel formation. The workflow also incorporates FAIR-compliant research data management to ensure transparent handling and long-term reusability of the time-resolved datasets. A schematic overview of the procedure is shown in Fig. 3.

Experimental design

A prerequisite for this protocol is the availability of proteins carrying complementary binding motifs that drive the self-assembly process. In our approach, these proteins are recombinantly produced in bacterial hosts and genetically engineered to include the desired motifs. We have applied the protocol to both covalent systems, such as SpyCatcher and SpyTag [13, 15], and non-covalent systems, including PDZ, GBD and SH3 domains [22]. Other self-assembly strategies can also be accommodated. When selecting an assembly strategy, note that very small oligomeric assemblies or weakly scattering systems may fall below the sensitivity range of standard benchtop DLS instruments. In addition, very fast assembly processes may exceed the effective temporal resolution of the workflow due to manual mixing and instrument initiation. Once suitable motifs have been selected, it is essential

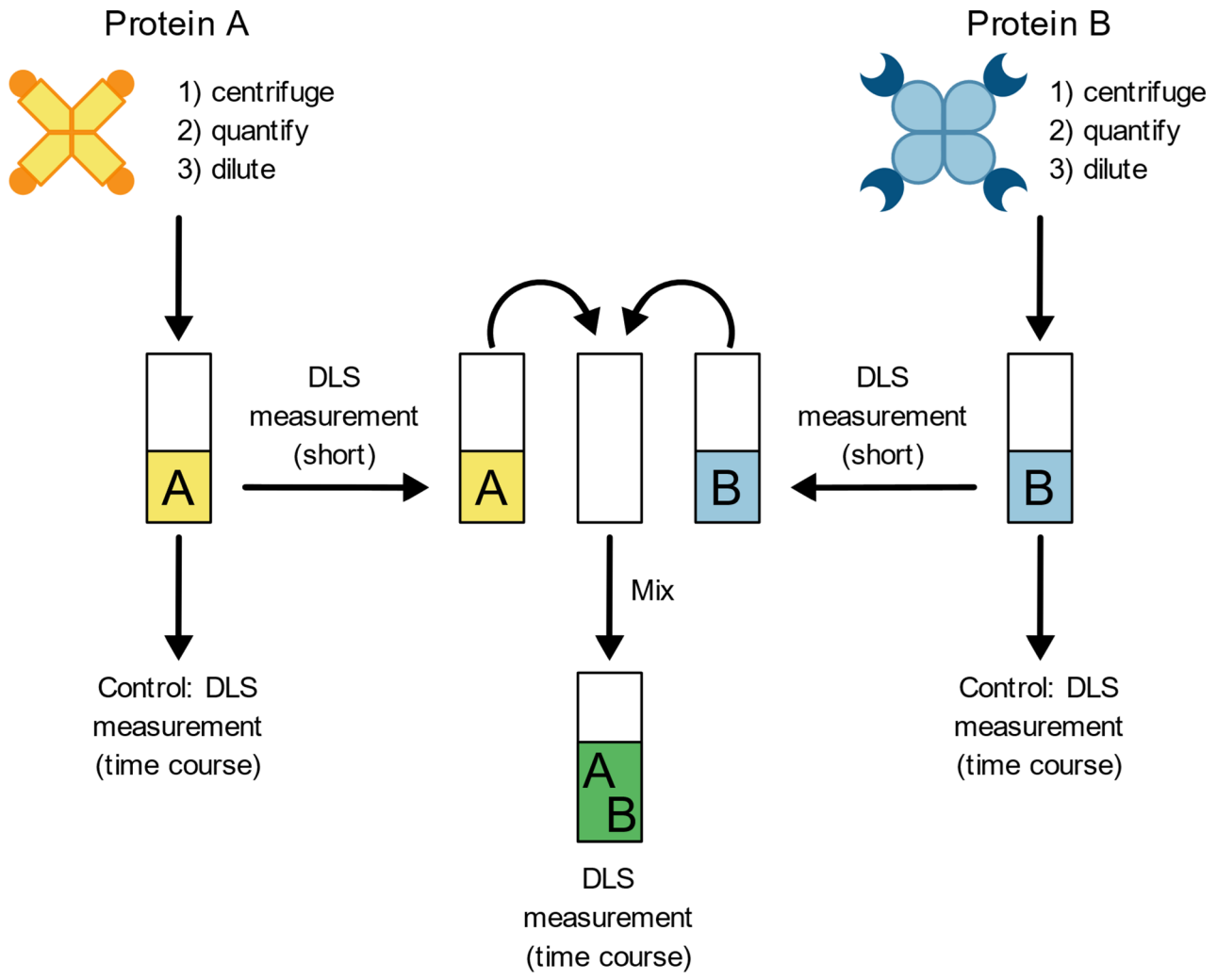

Fig. 3 Schematic representation of the procedure to monitor protein self-assembly by DLS, illustrating the sequential steps used to follow the assembly of two complementary proteins in solution. The procedure can be readily adapted to monitor the assembly of more than two proteins.

to verify that their incorporation does not compromise the structure or function of the protein. For enzymes intended for biocatalytic applications, this should be confirmed by comparing their catalytic activity in the absence and presence of the assembly motif to ensure that functionality is preserved after modification.

Another prerequisite is the identification of a buffer system in which the self-assembling proteins remain functional and stable without undergoing undesired aggregation over time. Practical guidelines for selecting buffer conditions suitable for proteins and protein complexes are available [32, 33]. In our work, we routinely use potassium phosphate buffer and, for simplicity, enter the viscosity and refractive index of water as the measurement parameters in the DLS instrument (Table 2). When working with buffers of substantially different viscosity or refractive index, these parameters should be determined or calculated at the experimental temperature to ensure accurate results.

In addition, several DLS measurement parameters require optimization, most importantly protein concentration and temperature. Scattering intensity in DLS measurements depends on both protein concentration and molecular weight. As a practical guideline, adequate signal-to-noise is typically obtained when the product of mass concentration and molecular weight (c·MW) is on the order of 10 kDa·g/L or higher on standard benchtop instruments. The proteins investigated here have molecular weights between approximately 24 and 40 kDa and adopt defined oligomeric quaternary structures (Table 1). While oligomerization does not affect the applicability of the c·MW guideline for estimating scattering signal, it is an important factor governing interaction valency and subsequent hydrogel network formation.

As shown in Fig. 2a, protein concentration strongly influences the kinetics of size increase: higher concentrations generally accelerate assembly and lead to larger particles. At the same time, concentrations above

Table 1 Molecular weights and oligomeric state of the proteins investigated.

Protein	MW / kDa	Quaternary Structure
GDH-ST	31	Tetramer
ADH-SC	40	Tetramer
GDH-PDZL	30	Tetramer
ADH-PDZB	38	Tetramer
GDH-SH3L	31	Tetramer
ADH-SH3B	35	Tetramer
GDH-GBDL	33	Tetramer
ADH-GBDB	37	Tetramer
PAD-ST2	24	Dimer
PAD-SC	33	Dimer

approximately 1 mM may compromise data quality because strong scattering and increased viscosity can interfere with reliable correlation analysis. The choice of temperature depends on both the assembly process and the stability of the proteins under investigation. In our case, we typically use 25–30 °C, consistent with the conditions employed in larger-scale syntheses of all-enzyme hydrogels for flow reactor applications.

Materials

Biological materials

- Individual self-assembling proteins purified to homogeneity.

Reagents

- Buffer for protein self-assembly — e.g., Sodium or Potassium Phosphate, Tris, HEPES, with NaCl or other additives.

Laboratory supplies

- Disposable micro cuvettes (Brand, cat. no. 759200; or Malvern Panalytical, cat. no. ZEN0040).
- Microcentrifuge tubes (Eppendorf, 0030121023).
- Cellulose acetate 0.2 µm syringe filters with luer adapter (Lab Lostistigy Group, 9.055 511).
- Disposable syringe 5 mL (B. Braun Omnifix, TZ-1409).

Laboratory equipment

- Benchtop DLS instrument. This protocol was performed with a Zetasizer Nano ZSP from Malvern Panalytical, but it can be easily adapted to equivalent DLS instruments.
- Benchtop refrigerated centrifuge (e.g. VWR® Micro Star 17R).
- UV/visible light spectrophotometer (e.g. Eppendorf, Biophotometer Plus UV/VIS).

Software or datasets

- DLS data acquisition software (in our case: Zetasizer software 8.02, Malvern Panalytical).
- Operating system: for the DLS measurements Microsoft Windows 10 or higher (depending on requirements of the manufacturer); for data analysis Linux, Windows or MacOS.

Biological material, reagent and equipment set-up

Protein preparation

- Produce proteins with complementary binding motifs following established production methods (see Introductory Chapter).
  CRITICAL STEP: Since DLS is highly sensitive to large particles, ensure that the proteins are at least 95% pure (for example via SDS-PAGE analysis) and that no high molecular weight contaminants are present. Protein samples that have been frozen and thawed may contain aggregates that interfere with DLS measurements. To minimize this risk, we recommend removing potential aggregates immediately before use by centrifuging the thawed samples or by passing the sample through a microfilter, for example a 0.2 µm cellulose acetate filter (see also the Troubleshooting section).

- The optimal amount of protein for the DLS measurements needs to be optimized (see Procedure). The minimum amount of protein needed for our standard procedure is 250 µL of each protein at 500 µM, but we recommend starting from protein stocks that are ≥ 1 mM.
  PAUSE POINT: if stable towards freezing and thawing, the proteins can be aliquoted and stored at − 80 °C for several months. We recommend flash-freezing in liquid nitrogen.

- The DLS cuvettes that we use require at least 40 µL of sample. However, to avoid air bubbles and facilitate the mixing steps, we normally use 80–100 µL of protein sample during measurements.

Buffer preparation

- Choose a buffer in which the proteins remain stable, meaning that they do not degrade or aggregate over time (see Experimental Design). Protein stability in the selected buffer can be assessed by DLS, as

described in the control measurements section (steps 14–21).
- Filter the experimental buffer through 0.2 µm syringe filters to remove dust and other particulate material from the solution, discarding the first drops from the filter. Collect the filtered buffer in clean microcentrifuge tubes.
- CRITICAL STEP: Since DLS is highly sensitive to large particles, filter the buffer fresh on the day of the measurements.

DLS instrument preparation

- Turn the instrument on, make sure the temperature is set to the temperature required during measurements (in our case, routinely 25 °C) and wait at least 30 min for the laser to stabilize.
- Set up the measurements in the DLS software according to the manufacturer's instructions. The parameters routinely used in our laboratory are listed in Table 2.

UV-vis preparation

- Turn the instrument on and wait at least 30 min for the lamps to stabilize.

Centrifuge preparation

- Turn the instrument on, set the temperature at the same temperature used during DLS measurements (in our case, routinely 25 °C) and wait for the temperature inside the centrifuge to stabilize.

Table 2 Instrument parameters for DLS measurements of proteins using a Zetasizer Nano ZSP from Malvern Panalytical with the Zetasizer software 8.02

Parameter		Value
Material		Protein (RI: 1.450; Absorption: 0.001)
Dispersant		Water (Viscosity: 0.8872 cP; RI: 1.330)
Temperature		As desired
Equilibration time (s)		0
Cell type		Disposable cuvettes (ZEN0040)
Measurement angle		173° Backscatter
Measurement duration		o Automatic for initial single protein measurements o 10 runs of 10 s during protein nanogel formation
Number of measurements		As required (≥ 3 for initial measurement)
Delay between measurements (s)		0
Positioning method		Seek for optimum position
Automatic attenuation selection		Yes
Analysis model		General purpose (normal resolution)
Mark-Houwink Parameters	A Parameter	0.428
	K Parameter (cm^2/s):	7.67e-05

Procedure

Protein sample preparation and initial quality controls

TIMING: 30 min

1. To check that the buffer is void of large particles, perform a short DLS measurement (3 repeated measurements) on 100 µL of buffer. The measurement should yield data of low quality or even an error message (e.g. low count rates).
2. (If applicable) thaw protein samples.
3. Centrifuge the protein samples at > 16,000 x g for 5 min at the temperature of the planned DLS measurements.
4. Transfer the supernatant to a new, clean microcentrifuge tube, leaving at least 5 µL of the original sample behind and taking care not to disturb or transfer any solid material or precipitated protein. CRITICAL STEP Although an appropriate buffer should minimize protein aggregation over time, avoid any unnecessary delay at this point and proceed quickly through the following steps to the nanogel self-assembly step (step 13).

5. Estimate the protein concentration by measuring the absorbance of a diluted protein sample (e.g. 100-fold) at 280 nm using the matching DLS buffer to zero the spectrophotometer. For accurate determination, ensure that the measured absorbance falls between 0.1 and 0.9 AU or adjust the protein dilution accordingly. The theoretical extinction coefficient can be calculated from the amino acid sequence of the protein (e.g., using ProtParam: [34] http://web.expasy.org/protparam/).
6. Any other protein concentration determination method is suitable, for example colorimetric methods such as the Lowry method, the bicinchoninic acid assay (BCA) or the biuret method [35].
7. The protein concentration used in the nanogel formation measurements can be optimized depending on the specific system under study. We routinely use 500 µM as a starting point and this concentration worked well for all the protein systems we investigated. Higher protein concentration normally yields faster kinetics of protein self-assembly, but can also lead to a lower quality of the DLS data during the assembly process.
8. Before performing a nanogel formation experiment, each individual protein is first investigated alone (Fig. 3). For this, prepare directly in a cuvette 100 µL of protein solution diluted in filtered buffer with a final

protein concentration of 500 μM (or as required after optimization).
CRITICAL STEP: Air bubbles can disrupt DLS measurements. Ensure that no bubbles are trapped at the bottom of the cuvette. Bubbles at the surface can be removed by bursting them with a sharp pipette tip or by gently applying air saturated with isopropanol (for example, from the headspace of an isopropanol squeeze bottle). If necessary, samples can be degassed prior to loading to further minimize the presence of air bubbles.

9. Perform at least three repeated DLS measurements on the individual proteins. The repeated measurements should have reproducible count rates and Z-average, and have a polydispersity index (PDI) < 0.7. Samples with PDI > 0.7 are considered not suitable for DLS. Built-in fitness features in the data analysis software (for example the 'Expert Advice' tab in in the Zetasizer software) can help evaluating the quality of the data.
CRITICAL STEP: Samples that show poor data quality already at the stage of the individual proteins are not suitable for subsequent self-assembly measurements. High PDI values, unstable count rates, or very low scattering intensity may indicate aggregation, sample heterogeneity, or weakly scattering systems such as very small oligomeric assemblies. See the Troubleshooting section for suggestions on how to improve sample quality.

10. Repeat the DLS measurements for all proteins that will assemble the nanogel.

Continous monitoring of the self-assembly reaction
TIMING: 2–3 h

11. Set up the DLS instrument so that, once started, it performs a sequence of repeated, identical measurements for at least 2 h. To ensure consistent measurement conditions across different time-course experiments, we manually set the measurement duration to 10 runs of 10 s each. Each individual measurement therefore lasts 100 s, with no waiting time between consecutive measurements.
CRITICAL STEP: After mixing the self-assembling proteins, DLS measurements must begin immediately. Before proceeding, ensure that the instrument is fully prepared and can be started with a single click. Time-resolved DLS analysis further assumes that dispersant viscosity remains constant throughout the measurement series. Approaching macroscopic gelation, very high protein concentrations, or late-stage network formation can increase viscosity and distort apparent size values or fit quality. If such effects are suspected, reduce protein concentration, shorten the measurement series, or restrict data analysis to earlier time points.

12. In a new cuvette, quickly mix the individually measured proteins at the appropriate stoichiometry to initiate nanogel formation. For example, for a 1:1 mixture of proteins A and B, combine 70 μL of A with 70 μL of B (Fig. 3). This yields a final total protein concentration of 500 μM, corresponding to 250 μM of each component. The volumes can be adjusted to meet other stoichiometric requirements. For optimal mixing, we recommend maintaining a final volume between 100 and 200 μL and avoiding pipetting volumes below 20 μL. Ensure that no air bubbles are present in the cuvette (see Critical Step in step 8).
13. Immediately start the series of DLS measurements and continue measuring for at least 2 h.
PAUSE POINT: If needed, the experiment can be paused at this stage, and the control measurements and data analysis can be performed the following day. The sample in the cuvette can be discarded. If self-assembly is driven by covalent bond formation, an SDS-PAGE analysis of the DLS sample (after appropriate dilution) should reveal a high-molecular-weight band corresponding to the conjugate (see also Expected results and Fig. 4).

Control DLS measurements
TIMING: 2–3 h per protein

14. To verify that the change in size observed during the self-assembly reaction is not due to protein aggregation, the individual proteins are monitored via DLS over extended time.

For each protein that participates in nanogel formation:

15. Repeat steps 1–7 of the procedure to obtain a fresh protein sample.
16. Prepare directly in a cuvette 100 μL of protein solution diluted in filtered buffer with a final protein concentration of 500 μM (or as required after optimization of the self-assembly reaction, see Experimental Design). Ensure that no air bubbles are present in the cuvette (see Critical Step in step 8).
17. Perform at least three repeated DLS measurements on the protein. The repeated measurements should have reproducible count rates and Z-average, and have a polydispersity index (PDI) < 0.7. The results should be comparable to what was obtained at step 9.

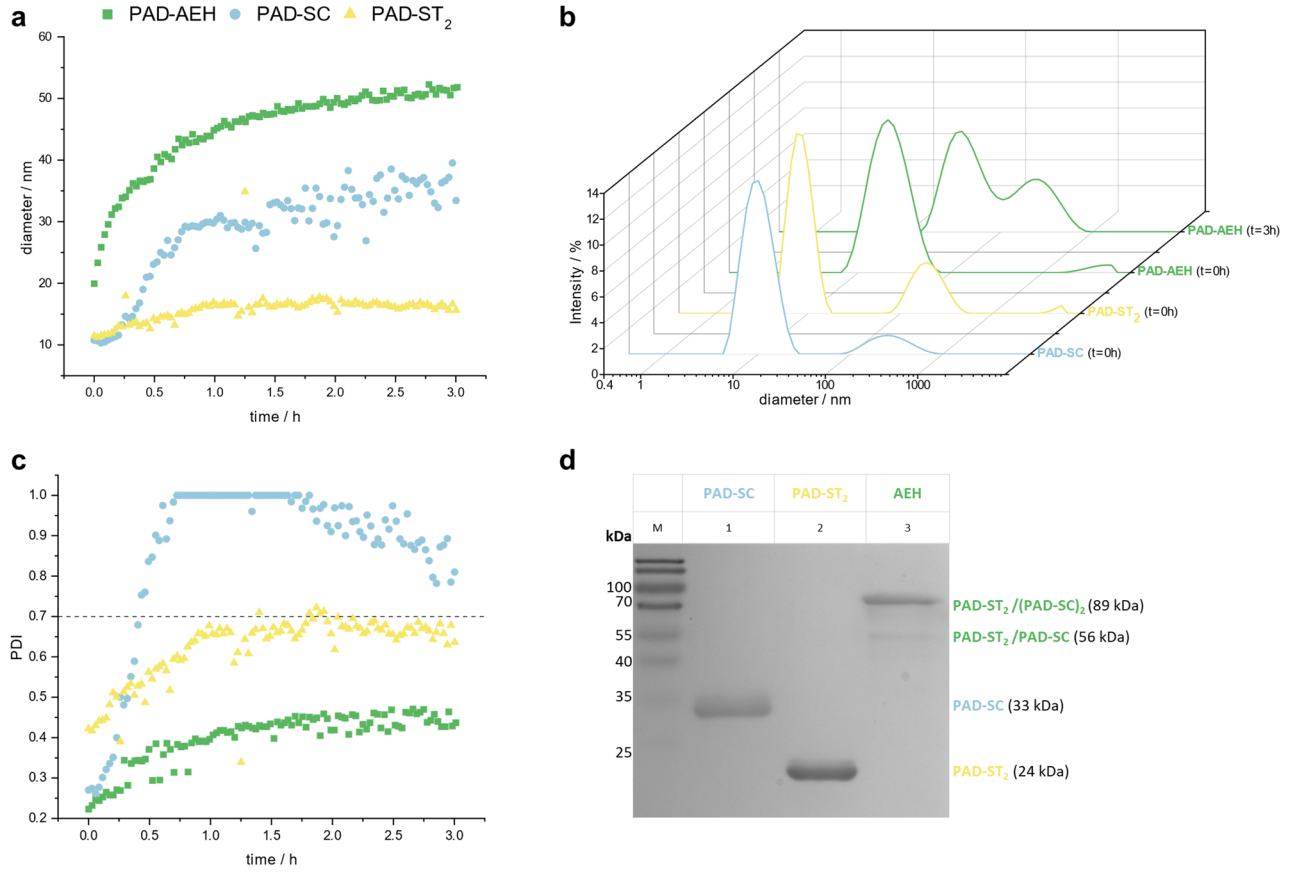

Fig. 4 Exemplary data evaluation using monomodal (method A) and multimodal (method B) analyses for the self-assembly of phenolic acid decarboxylase variants PAD-SC and PAD-ST$_2$. (**a**) Time-dependent hydrodynamic diameter (Z-average) for a 2:1 mixture of PAD-SC and PAD-ST$_2$ recorded by 10 sequential steps of 10 measurements each at 25 °C (see also the trouble shooting section); the mixed sample is shown in green, and the corresponding individual proteins are shown in blue (PAD-SC) and yellow (PAD-ST$_2$). The initial particle growth rate, obtained by linear regression of the early time points, is 1.37 nm per minute. (**b**) Intensity size distributions of the initial time points (t = 0 h) for the individual proteins and the final time point of the assembled nanogel (PAD-AEH at t = 3 h), illustrating changes in particle size distribution over time. (**c**) Time-dependent polydispersity index (PDI) for the same samples, used as a quality metric for method A; values above 0.7 indicate reduced data quality. Panels a and c report diameter and PDI values obtained from monomodal (cumulant) analysis, whereas panel b shows intensity-weighted particle size distributions derived from multimodal analysis. (**d**) SDS-PAGE analysis of protein samples (2 µg) taken after DLS measurements, showing PAD-SC (33 kDa, lane 1), PAD-ST$_2$ (24 kDa, lane 2), and the two conjugates formed upon assembly, PAD-ST$_2$/PAD-SC (56 kDa) and PAD-ST$_2$/(PAD-SC)$_2$ (89 kDa, lane 3).

18. As in the self-assembly reaction, set up the DLS instrument so that, once started, it performs a sequence of repeated, identical measurements for at least 2 h. To ensure consistent measurement conditions across all time-course experiments, we manually set the measurement duration to 10 runs of 10 s each. Each individual measurement therefore lasts 100 s, with no waiting time between consecutive measurements.
19. Start the series of DLS measurements and continue measuring for at least 2 h.
20. Repeat steps 14–19 for each protein that participates in nanogel formation.
21. The particle size during the DLS measurement of the individual proteins should not increase significantly. If this happens, see Troubleshooting section.

Data evaluation and analysis

Modern DLS software packages provide several algorithms to extract particle size information from the autocorrelation function. Two principal approaches are used: (A) monomodal distribution analysis and (B) multimodal distribution analysis. In method A, also referred to as cumulant analysis [36], a single exponential is fitted to the autocorrelation function, yielding an average hydrodynamic diameter (Z-average) and an estimate of the distribution width, expressed as the polydispersity index (PDI). Note that the definition and range of the PDI may vary between software packages; in the Zetasizer software used here, PDI values range from 0 to 1. Cumulant analysis is the preferred method for monodisperse samples.

In method B, multiple exponentials are fitted to the autocorrelation function to generate an intensity-based

distribution of particle sizes with different hydrodynamic radii. This approach is suitable for samples that are not monodisperse, although samples with very high polydispersity remain difficult to analyze reliably using DLS. Most DLS software packages can perform both monomodal and multimodal analyses. The choice of which approach to report for a given self-assembly experiment depends on the quality of the raw data and the fit, as described in the steps below.

Data evaluation method A: Z-average increase over time (monomodal distribution)

The most straightforward way to determine the nanogel growth profile is to plot the Z-average hydrodynamic diameter, which represents an intensity-weighted estimate of particle size, as a function of measurement time. This cumulant-based (monomodal) analysis is appropriate only for samples that exhibit a monomodal size distribution and for which the autocorrelation function decays fully to unity at long delay times. Importantly, a monomodal size distribution does not imply a monodisperse sample, but rather that a single dominant diffusive mode is present. Polydispersity indices derived from cumulant analysis are therefore meaningful only under these conditions and should not be used as sole data-quality criteria for samples exhibiting multiple decay modes. If the autocorrelation function cannot be adequately described by a single exponential or does not return close to unity, analysis using multiple exponentials or regularization-based distribution methods (Data evaluation method B) is required. When these criteria are fulfilled, Z-average growth profiles can be obtained as described in steps Ai–Avii below.

Ai. Using the advice tool available within the measurement software (e.g. 'expert advice' in the Zetasizer software), inspect the quality of the DLS measurements in the time course.

Aii. If the fit error for the Cumulant analysis is too high (for our version of the Zetasizer software this means > 0.005) for many of the measurements, we suggest to plot the intensity size distribution instead (method B below).
Note: the PDI value for some measurements in the time course might be > 0.7. This is normal as the formation of nanogel particles will inherently increase the polydispersity of the sample. PDI values and corresponding thresholds depend on the software and instrument used for DLS analysis; the values reported here refer to the implementation of the software used in this study. We suggest also plotting the PDI over time (step A-vii below).

Aiii. Export the data and measurement parameters from the proprietary software as quantitative tabular data (see also ii in the Data management section).

Aiv. Using a spreadsheet editor (we use Microsoft Excel 2019 and OriginPro 2023), scripts or another preferred method of choice, calculate for each measurement the elapsed time from the beginning of the time course, using the timestamps associated with each measurement.

Av. Plot the Z-average (diameter) as a function of the elapsed time as a scatter plot. As a size comparison, add to the plot the Z-average measured for the individual proteins at the beginning of the experiment.
CRITICAL POINT: If some measurements were flagged for a failed cumulant analysis, the associated Z-average data-points might appear as almost outliers in the plot. We once again remind the reader that no reliable size information should be derived from these Z-average values.

Avi. To discriminate between non-specific protein aggregation and self-assembly, compare the Z-average evolution over time for the self-assembly reaction with the data on the individual proteins measured during the control experiments.

Avii. For further understanding of the assembly process, plot also PDI values as a function of the elapsed time as a scatter plot for both the assembly reaction and the control experiments. This evaluation can be particularly useful if the control experiments show some size increase for the individual proteins to further understand the process (see also Troubleshooting section and the expected results in Fig. 4).

Data evaluation method B: intensity size distribution changes over time (multimodal distribution)

When the cumulant-based (monomodal) analysis is not applicable, for example because the autocorrelation function cannot be adequately described by a single exponential or does not decay fully to unity, particle size information should be extracted using distribution-based analyses. In such cases, regularization or multi-exponential fitting yields an intensity-weighted size distribution that can reveal the presence of multiple particle populations contributing significantly to the scattering signal. This approach is particularly suitable for multimodal systems and is described in steps Bi to Bv below.

Bi. Using the quality metrics provided by the measurement software (for example, inspection of the autocorrelation function and associated diagnostics), assess the quality of the DLS measurements across the time course.

Bii. If the quality of the distribution-based analysis is not satisfactory, for example due to excessive noise or unstable correlation functions, the resulting size distributions should not be interpreted further. See the Troubleshooting section for suggestions on how to improve sample quality.

Biii. Export the raw data for the intensity size distribution from the proprietary software as quantitative tabular data (see also ii in the Data management section).

Biv. Using a spreadsheet editor, scripts or another preferred method of choice, plot the intensity percentages (y) as a function of the size (x, log10 scale) and the elapsed time from the first measurement (z) as a waterfall plot.

Bv. To discriminate between non-specific protein aggregation and self-assembly, compare the waterfall plot for the self-assembly reaction with the corresponding plots obtained for the individual proteins in the control experiments. The appearance of additional peaks or shifts in intensity contributions over time can indicate the emergence of distinct particle populations during assembly.

Data management

To contribute to the reproducibility, transparency and long-term usability of experiments, we recommend storing, analyzing and managing the data generated by the DLS measurements in accordance with F.A.I.R. (Findable, Accessible, Interoperable, and Reusable) principles (https://www.go-fair.org/fair-principles/). This includes:

i. Accompany the raw data with rich metadata necessary for someone to understand the data (including when the measurement was performed, instrument type and software, identifiers of the proteins and mention of any artificial modification, buffer composition, concentration of the proteins, protocol used etc.). We recommend following the STRENDA guidelines (https://www.beilstein-strenda-db.org/strenda/public/guidelines.xhtml). Even if they were originally designed for enzyme activity assays, we find that these guidelines can easily be adopted for this protocol with minimal modifications.

ii. DLS data are typically recorded and analyzed using proprietary software provided by the instrument manufacturer. Export and save the raw data from these proprietary file formats into open, quantitative tabular formats such as comma-separated values (.csv) or tab-delimited files (.tab). Be aware that, when using default export settings, some software may omit useful parameters or raw data, for example fit errors or the values required to plot intensity size distributions. Most DLS software packages allow customization of export settings, and these should be adjusted to ensure that all relevant information is included.

iii. Upload the metadata, the raw data, and the analyzed data to a suitable data repository, in accordance with the regulations of your institution and funding agencies, and following the instructions and requirements of the chosen repository. Suitable examples include general-purpose repositories such as Zenodo, Figshare, and Dryad, or institutional repositories such as KITopen. Assign a digital object identifier (DOI) to the deposited dataset.

As an example, we made the data discussed in the expected results section (Figs. 2c-e and 4), including the raw data and metadata file, available also in the KITopen repository with Datasets.

General notes and troubleshooting

Problem: poor data quality in initial DLS measurements (step #9)

If the quality of the initial DLS measurements of the individual proteins is not satisfactory, this is most often due to polydispersity in the solution, typically caused by protein aggregates. While repeated centrifugation can remove larger aggregates, it may be insufficient to eliminate small aggregate species. We therefore recommend filtering samples through at least a 0.22 µm membrane prior to DLS measurements. Where compatible with protein concentration and sample properties, finer filters (for example 0.1 µm) may further improve data quality; however, for highly concentrated protein solutions, filter clogging may limit the use of smaller pore sizes. Individual protein samples should ideally exhibit a monomodal size distribution with low polydispersity prior to self-assembly measurements; however, acceptable thresholds depend on protein concentration, instrument sensitivity, and analysis software. In this work, samples with PDI values below approximately 0.7 were considered suitable for subsequent assembly experiments. If these steps do not improve data quality, the protein preparation should be revisited. Possible measures include optimizing the buffer composition for measurement and storage (see Experimental Design), adding a size-exclusion chromatography step to the purification workflow, or avoiding freezing and thawing of the sample.

Poor data quality can also result from very weak scattering intensity or unstable count rates, which may occur for very small oligomeric assemblies or low-molecular-weight complexes that fall below the sensitivity range of standard benchtop DLS instruments. In cases of weak scattering or persistently unstable count rates, increasing protein concentration within the linear range of

the detector or extending measurement duration may improve signal-to-noise ratio; however, if reliable data quality cannot be achieved despite optimization, the system may not be suitable for DLS-based analysis under the chosen conditions.

Problem: size increase during the control measurements (step #21)

If the hydrodynamic diameter of the individual protein increases significantly over time during the control DLS measurements, this indicates protein aggregation. To mitigate this, the buffer composition should be optimized (see Experimental Design) or the measurement temperature should be reduced. We recommend performing a comprehensive buffer screening prior to self-assembly experiments, including variation of the pH. Commonly used buffers include MES, MOPS, phosphate, HEPES, Tris, and glycine. These can be supplemented with salt (for example 100 to 1000 mM NaCl) or stabilizing additives such as trehalose or L-arginine and L-glutamic acid [33, 37]. The screening process can be accelerated by parallelization using a microplate DLS device.

CRITICAL POINT: The measurements for the self-assembly reaction must also be repeated using the newly selected buffer or temperature.

Even if some protein aggregation is observed during the control experiments, analysis of the evolution of the PDI over time (step A-vii) in both the self-assembly reaction and the controls can provide insight into the processes underlying the observed increase in particle size (see also the expected results in Fig. 4).

Problem: poor data quality DLS measurements of self-assembly reaction (Data evaluation step Bii)

If the quality of the DLS measurements during the self-assembly reaction is not satisfactory, this is most often due to high polydispersity in the sample. If the individual proteins already exhibited high polydispersity, follow the recommendations provided above for troubleshooting step 9. If the high polydispersity is an inherent consequence of the self-assembly process, improved data quality may be obtained by reducing the protein concentration by a factor of two to five.

In addition, as particle size increases during the self-assembly reaction, the amount of light reaching the detector may rise beyond the optimal range, leading to an inappropriate attenuator setting. The instrument normally selects the attenuator automatically at the beginning of the measurement series, but it does not update this setting continuously. In some experiments, such as the PAD-AEH assembly, the count rate increased substantially after the first few measurements, indicating that the initially selected attenuator was no longer suitable. This is typically highlighted in the expert advice section of the software.

To prevent this problem, we recommend creating a measurement file (SOP) that contains the parameters listed in Table 2 for a block of 10 consecutive measurements. This SOP can be executed repeatedly (using the SOPPlayer in the Zetasizer software) to generate a continuous time course. When the SOP restarts after each block of 10 measurements, the attenuator is recalculated automatically, ensuring that the detector is not overloaded. This approach prevents errors caused by excessively high count rates and maintains consistent measurement quality throughout the entire self-assembly reaction.

Expected results

To illustrate expected results, we provide raw and analyzed DLS data corresponding to Fig. 2c, d and e. In these experiments, the assembly of two tetrameric enzymes, alcohol dehydrogenase (ADH) and glucose dehydrogenase (GDH), each equipped with complementary binding motifs (PDZ, SH3, or GBD), was monitored following the protocol described in this work. The high quality of the measurements allowed the use of the monomodal distribution (Data evaluation method A), enabling time-resolved visualization of the increase in hydrodynamic diameter as a function of the time elapsed after mixing. As the Z-average represents an intensity-weighted hydrodynamic diameter, the values reported here should be interpreted as comparative indicators of nanogel growth rather than as precise particle sizes, particularly for polydisperse systems. Plotting together the Z-average values of the assembly reaction and of the individual proteins (which remain stable over time) provides a direct comparison and highlights that the increase in particle size is due to nanogel formation rather than unspecific aggregation.

The three non-covalent systems shown in Fig. 2c, d and e illustrate characteristic differences in assembly behavior. The PDZ and SH3 systems display clear growth profiles, with SH3 assembling more rapidly and reaching larger particle sizes, consistent with their differing binding affinities. In contrast, the GBD system shows a considerably slower increase in hydrodynamic diameter (Fig. 2e). The unexpected increase in signal for one of the isolated proteins, GDH-GBDL (turquoise curve), may indicate unspecific aggregation of this component under the given assay conditions. While the underlying molecular cause cannot be conclusively assigned based on DLS data alone, this example demonstrates that deviations in the behavior of individual components, potentially arising from factors such as insufficient structural stability during prolonged incubation, can be readily detected using this protocol.

In addition to these non-covalent systems, we provide a second example illustrating data evaluation with both monomodal (method A) and multimodal (method B) approaches. This dataset corresponds to the self-assembly of a dimeric phenolic acid decarboxylase (PAD) fused to SpyCatcher (PAD-SC) and SpyTag (PAD-ST_2) [17], shown in Fig. 4. The time-resolved hydrodynamic diameter (method A) reveals the typical profile of covalent nanogel formation, with rapid particle growth followed by a plateau after approximately one hour (Fig. 4a, green). The individual proteins show different tendencies to aggregate, with PAD-ST_2 remaining relatively stable and PAD-SC showing behavior consistent with pronounced aggregation (yellow and blue curves, respectively).

Inspection of the time-resolved polydispersity index (PDI) further clarifies these observations: PAD-ST_2 remains below a PDI of 0.7, while PAD-SC displays a substantial increase over time, yielding soon data not suitable anymore for cumulant analysis and displaying for the PDI the upper limit value of 1. In contrast, the PDI of the assembled PAD-SC and PAD-ST_2 mixture increases during the early stages of nanogel formation but then stabilizes at approximately 0.45 (Fig. 4c), indicating a more uniform particle population than the individual components. This highlights that in this case self-assembly can reduce rather than amplify aggregation, underscoring the importance of including PDI plots alongside hydrodynamic diameter for correct data interpretation.

For comparison, the same dataset was evaluated using a multimodal distribution (method B). The evolution of the intensity size distribution is shown as a waterfall plot (Fig. 4b), where each trace represents a different time point. The traces from the individual proteins at t = 0 h and from the fully formed gel at t = 3 h illustrate the shift from smaller, broader species to larger, more defined assemblies. Even when the monomodal distribution provides sufficiently high-quality data, inspection of the intensity size distribution can reveal additional features, such as multimodality or heterogeneity in intermediate states. Finally, for covalent systems such as PAD-SC and PAD-ST_2, SDS-PAGE analysis of samples collected after each DLS measurement (Fig. 4d) confirms the formation of higher molecular weight conjugates corresponding to the expected assembly products. This verification step is not applicable to non-covalent interaction modules.

A useful parameter for describing nanogel formation is the initial particle growth rate, which quantifies the increase in hydrodynamic diameter during the early phase of assembly. This rate can be obtained by performing a linear regression on the initial portion of the time course where the Z-average increases approximately linearly. To determine the initial growth rate, the following general procedure can be applied: (i) identify the early region of the curve in which the increase in Z-average is monotonic and visually linear, (ii) select a time window that captures this linear regime while excluding the earliest noisy points and any later curvature or plateau, and (iii) perform a least-squares linear regression on the selected data points. The slope of this regression corresponds to the initial particle growth rate, expressed as the change in Z-average per unit time. Applying this approach allows comparison of assembly kinetics across different systems using consistent and quantitative metrics.

For the systems shown in Fig. 2c, d and e, linear regression of the early time points yielded initial particle growth rates of 0.12 nm per minute, 1.97 nm per minute, and 0.06 nm per minute, respectively. Significant differences were observed between the interaction modules. The SH3 system exhibited the fastest and most pronounced nanogel formation, reaching an average particle size of 33 nm. The PDZ system formed particles more slowly, with an initial rate of 0.12 nm per minute and an average size of approximately 22 nm. In contrast, the GBD system displayed a considerably slower increase of 0.06 nm per minute, resulting in an average particle size of only 18 nm. These endpoint sizes reflect not only the intrinsic binding strengths of the interaction modules but also the effective multivalency and geometric accessibility of the domains once fused to the enzyme scaffolds. Faster early growth therefore tends to correlate with, but does not exclusively determine, the final particle size.

Compared to covalent assembly via the SC and ST system, which displays an initial growth rate of approximately 1.37 nm per minute and a particle size of about 50 nm [13], the non-covalent systems generally showed slower growth, with the exception of the SH3 pair. These results are consistent with the overall trend that covalent interactions drive faster and more extensive network formation than non-covalent ones. The larger particle size of the covalent SC/ST system likely reflects the irreversible nature of isopeptide bond formation, which promotes continued network expansion.

However, the order of the observed particle growth rates does not strictly follow the expected trend based solely on reported binding affinities (SH3 > GBD > PDZ). This deviation suggests that the assembly behavior of these enzyme-based systems is shaped by additional factors introduced by fusion of the interaction domains to the enzyme scaffolds. Multivalent contacts inherent to the tetrameric architecture, as well as steric constraints or solvation effects, may influence the accessibility and effective orientation of the binding domains. Such factors can modulate both the assembly kinetics and the final nanogel size, explaining why particle diameters do not always scale directly with affinity or early growth rate.

It should be emphasized that the quantitative descriptors obtained from this protocol, including initial particle

growth rates and apparent hydrodynamic diameters, provide a comparative characterization of assembly behavior rather than direct mechanistic insight. While qualitative trends between assembly kinetics, final particle size, and reported binding affinities may be observed, these relationships are system dependent and cannot be interpreted as direct causal correlations based on DLS data alone. DLS measurements report intensity-weighted hydrodynamic sizes and capture the evolution of assemblies in solution, but additional orthogonal approaches would be required to unambiguously resolve the underlying molecular mechanisms. Accordingly, the parameters reported here should be interpreted as quantitative descriptors for comparing assembly systems and conditions, rather than as definitive measures of binding interactions.

Taken together, the protocol enables robust and reproducible quantification of nanogel formation across a wide range of protein assembly systems. By providing standardized access to time-resolved growth profiles and apparent particle sizes, it facilitates systematic comparison of interaction modules, protein variants, and experimental conditions, and supports informed optimization of self-assembling biomolecular materials.

Acknowledgements
We thank Cornelia Ziegler for experimental help.

Author contributions
Conceptualization: M.A.M, K.S.R, C.M.N; Methodology: M.A.M.; Investigation: A.W., J.S.H; Formal analysis: M.A.M, A.W, A.J.W., J.K., J.S.H; Writing – original draft: M.A.M, C.M.N; Writing – review & editing: A.W, A.J.W., J.K., K.S.R, C.M.N;. All authors reviewed and approved the manuscript.

Funding
Open Access funding enabled and organized by Projekt DEAL. This work was supported through the Helmholtz program "Materials Systems Engineering" under the topic "Adaptive and Bioinstructive Materials Systems" (43.33.11). A.J.W. is grateful for support by a Kekulé fellowship by Fonds der Chemischen Industrie (FCI).

Data availability
The datasets generated and used during the current study are available in the KITopen repository, [Datasets] (https://doi.org/10.35097/zaskz3ddmtnd287k).

Declarations

Ethics approval and consent to participate
Not applicable.

Consent for publication
Not applicable.

Competing interests
The authors declare no competing interests.

Received: 24 November 2025 / Accepted: 14 March 2026
Published online: 13 May 2026

References

1. Solomonov A, Kozell A, Shimanovich U. Designing Multifunctional Biomaterials via Protein Self-Assembly. Angew Chem Int Ed. 2024;63(14):e202318365.
2. Gou Y, Wang A, Ding L, Yang X, Lu X, Qi Q, et al. A Comprehensive Review on Protein-Based Hydrogels: From Structure Modification to Applications. ChemistrySelect. 2025;10(14):e202405618.
3. Sheldon RA, Woodley JM. Role of Biocatalysis in Sustainable Chemistry. Chem Rev. 2018;118(2):801–38.
4. Bell EL, Finnigan W, France SP, Green AP, Hayes MA, Hepworth LJ, et al. Biocatal Nat Rev Methods Primers. 2021;1(1):46.
5. Wu S, Snajdrova R, Moore JC, Baldenius K, Bornscheuer UT. Biocatalysis: Enzymatic Synthesis for Industrial Applications. Angew. Chem. Int. Ed. 2001;113:3443–3453. 2021;60(1):88–119.
6. Buller R, Lutz S, Kazlauskas RJ, Snajdrova R, Moore JC, Bornscheuer UT. From nature to industry: Harnessing enzymes for biocatalysis. Science. 2023;382(6673):eadh8615.
7. Kuchler A, Yoshimoto M, Luginbuhl S, Mavelli F, Walde P. Enzymatic reactions in confined environments. Nat Nanotechnol. 2016;11(5):409–20.
8. France SP, Hepworth LJ, Turner NJ, Flitsch SL. Constructing Biocatalytic Cascades: In Vitro and in Vivo Approaches to de Novo Multi-Enzyme Pathways. ACS Catal. 2017;7(1):710–24.
9. Rabe KS, Muller J, Skoupi M, Niemeyer CM. Cascades in Compartments: En Route to Machine-Assisted Biotechnology. Angew Chem Int Ed. 2017;56(44):13574–89.
10. Woodley JM. Accelerating the implementation of biocatalysis in industry. Appl Microbiol Biotechnol. 2019;103(12):4733–9.
11. Ellis GA, Klein WP, Lasarte-Aragones G, Thakur M, Walper SA, Medintz IL. Artificial Multienzyme Scaffolds: Pursuing in Vitro Substrate Channeling with an Overview of Current Progress. ACS Catal. 2019;9(12):10812–69.
12. Du P, Xu S, Xu Z-K, Wang Z-G. Bioinspired Self-Assembling Materials for Modulating Enzyme Functions. Adv Funct Mater. 2021;31(38):2104819.
13. Peschke T, Bitterwolf P, Gallus S, Hu Y, Oelschlaeger C, Willenbacher N, et al. Self-Assembling All-Enzyme Hydrogels for Flow Biocatalysis. Angew Chem Int Ed. 2018;57(52):17028–32.
14. Reddington SC, Howarth M. Secrets of a covalent interaction for biomaterials and biotechnology: SpyTag and SpyCatcher. Curr Opin Chem Biol. 2015;29:94–9.
15. Bitterwolf P, Gallus S, Peschke T, Mittmann E, Oelschlaeger C, Willenbacher N, et al. Valency engineering of monomeric enzymes for self-assembling biocatalytic hydrogels. Chem Sci. 2019;10(42):9752–7.
16. Bitterwolf P, Ott F, Rabe KS, Niemeyer CM. Imine Reductase Based All-Enzyme Hydrogel with Intrinsic Cofactor Regeneration for Flow Biocatalysis. Micromachines. 2019;10(11):783.
17. Mittmann E, Gallus S, Bitterwolf P, Oelschlaeger C, Willenbacher N, Niemeyer CM, et al. A Phenolic Acid Decarboxylase-Based All-Enzyme Hydrogel for Flow Reactor Technology. Micromachines. 2019;10(12):795.
18. Peschke T, Bitterwolf P, Hansen S, Gasmi J, Rabe KS, Niemeyer CM. Self-Immobilizing Biocatalysts Maximize Space–Time Yields in Flow Reactors. Catalysts. 2019;9(2):164.
19. Peschke T, Bitterwolf P, Rabe KS, Niemeyer CM. Self-Immobilizing Oxidoreductases for Flow Biocatalysis in Miniaturized Packed-Bed Reactors. Chem Engin Technol. 2019;42(10):2009–17.
20. Bitterwolf P, Zoheir AE, Hertel J, Kröll S, Rabe KS, Niemeyer CM. Intracellular Assembly of Interacting Enzymes Yields Highly-Active Nanoparticles for Flow Biocatalysis. Chem Eur J. 2022;28(66):e202202157.
21. Hertel JS, Bitterwolf P, Kröll S, Winterhalter A, Weber AJ, Grösche M, et al. Biocatalytic Foams from Microdroplet-Formulated Self-Assembling Enzymes. Adv Mater. 2023;35(39):2303952.
22. Hertel JS, Martini MA, Stoeckle M, Weber AJ, Rabe KS, Niemeyer CM. Harnessing Non-Covalent Protein–Protein Interaction Domains for Production of Biocatalytic Materials Systems. Adv Funct Mater. 2025;35:e13931.
23. Falke S, Betzel C. Dynamic Light Scattering (DLS). In: Pereira AS, Tavares P, Limão-Vieira P, editors. Radiation in Bioanalysis: Spectroscopic Techniques and Theoretical Methods. Cham: Springer International Publishing; 2019. pp. 173–93.
24. Minton AP. Recent applications of light scattering measurement in the biological and biopharmaceutical sciences. Anal Biochem. 2016;501:4–22.
25. Lorber B, Fischer F, Bailly M, Roy H, Kern D. Protein analysis by dynamic light scattering: Methods and techniques for students. Biochem Mol Biol Educ. 2012;40(6):372–82.

26. Yuan W, Dong G-Z, Ning H, Guan X-X, Dong Y-C. Applying dynamic light scattering to investigate the self-assembly process of DNA nanostructures. Chin Chem Lett. 2024;35:108384.
27. Dierks K, Meyer A, Einspahr H, Betzel C. Dynamic Light Scattering in Protein Crystallization Droplets: Adaptations for Analysis and Optimization of Crystallization Processes. Cryst Growth Des. 2008;8(5):1628–34.
28. Liu XY, Tsukamoto K, Sorai M. New Kinetics of CaCO3 Nucleation and Microgravity Effect. Langmuir. 2000;16(12):5499–502.
29. Gast K, Nöppert A, Müller-Frohne M, Zirwer D, Damaschun G. Stopped-flow dynamic light scattering as a method to monitor compaction during protein folding. Eur Biophys J. 1997;25(3):211–9.
30. Dueber JE, Wu GC, Malmirchegini GR, Moon TS, Petzold CJ, Ullal AV, et al. Synthetic protein scaffolds provide modular control over metabolic flux. Nat Biotechnol. 2009;27(8):753–9.
31. Connolly Brian D, Petry C, Yadav S, Demeule B, Ciaccio N, Moore Jamie MR, et al. Weak Interactions Govern the Viscosity of Concentrated Antibody Solutions: High-Throughput Analysis Using the Diffusion Interaction Parameter. Biophys J. 2012;103(1):69–78.
32. Houser J, Kosourova J, Kubickova M, Wimmerova M. Development of 48-condition buffer screen for protein stability assessment. Eur Biophys J. 2021;50(3):461–71.
33. Tekewe A, Connors NK, Sainsbury F, Wibowo N, Lua LHL, Middelberg APJ. A rapid and simple screening method to identify conditions for enhanced stability of modular vaccine candidates. Biochem Eng J. 2015;100:50–8.
34. Gasteiger E, Hoogland C, Gattiker A, Duvaud Se, Wilkins MR, Appel RD, et al. Protein Identification and Analysis Tools on the ExPASy Server. In: Walker JM, editor. The Proteomics Protocols Handbook. Totowa, NJ: Humana; 2005. pp. 571–607.
35. Krohn RI. The Colorimetric Detection and Quantitation of Total Protein. Curr Protocols Cell Biology. 2002;15(1):AH31–328.
36. Koppel DE. Analysis of Macromolecular Polydispersity in Intensity Correlation Spectroscopy: The Method of Cumulants. J Chem Phys. 1972;57(11):4814–20.
37. Golovanov AP, Hautbergue GM, Wilson SA, Lian L-Y. A Simple Method for Improving Protein Solubility and Long-Term Stability. J Am Chem Soc. 2004;126(29):8933–9.

Publisher's note